High-Temperature Phase of $MgSiF_6 \cdot 6H_2O$ by EPR of Manganese Ions

Wlodzimierz Zapart*

Institute of Physics, Technical University, 42-200 Czestochowa, Al. Armii Krajowej 19, Poland

Received: February 27, 2002; In Final Form: November 21, 2002

The paper deals with the interpretation of the Mn^{2+} EPR spectra in the high-temperature phase of $MgSiF_6 \cdot 6H_2O$. Two models are presented: the continuous and the discrete antiphase domain walls. Just above the ferroelastic phase transition, for each resonance transition two EPR lines are observed: the broad one and the narrow one. It is shown that the narrow line originates from centers lying inside the domains whereas the broader originates from the centers lying inside the domain walls.

Introduction

Modulated (commensurate and incommensurate) structures form an important class of structures observed among all categories of materials. The modulations can involve a continuous variable (for example, the atomic position in the case of displacive modulations) or a discrete variable that takes a finite number of values (long-period antiphase boundary structures). Two kinds of models have been proposed for antiphase boundary (APB) structures: the first assuming sharp domain walls strictly contained in crystal planes,[1] and the second taking into account wavy antiphase boundaries.[2]

These structures can be studied within the general Landau-Ginzburg theory of phase transitions.[3] In this framework they consist of commensurate regions separated by discommensurations or solitons. These solitons can correspond to the wide antiphase boundaries at high temperatures. At lower temperatures the solitons become narrower and pinned to the lattice so that commensurate structures can appear through a lock-in transition. At intermediate temperatures, complex structures can appear with the possible occurrence of a devil's staircase.[3] The structures can all be described using more or less smoothed square wave functions with the smoothing being a function of temperature.

In crystals belonging to a family of the type $ABF_6 \cdot 6H_2O$ the existence of regular antiphase domain structure has been reported in their high-temperatures phases.[4] The EPR spectra of admixture ions observed in this temperature range resemble those seen in the incommensurate systems.[5] In this paper ,we show that two kinds of manganese centers contribute to the EPR spectrum just above the phase transition temperature, which results in the splitting of each EPR line into two component lines. One of these lines originates from centers located inside the domains and the second one from centers located within the domain walls. The above description of the EPR spectrum is consistent with the structural model of the high-temperature phase of $MgSiF_6 \cdot 6H_2O$ as presented in the paper.[4]

The Structure of the High-Temperature Phase of $MgSiF_6 \cdot 6H_2O$

Magnesium fluosilicate hexahydrate $MgSiF_6 \cdot 6H_2O$ (MFSH) belongs to a crystal family of the type $ABF_6 \cdot 6H_2O$ where A is a divalent iron group metal ion (Fe, Co, Ni, Zn, Mn, Mg) and B is a quadrivalent element very much like Si, Sn, Ti, Ge. The $ABF_6 \cdot 6H_2O$ system is of interest since most of its members undergo structural phase transitions below room temperature which have been investigated by different macroscopic and microscopic methods.[5−13] The rhombohedrally distorted CsCl-type structure of these compounds is made up of columns with alternating$[A(H_2O)_6]^{2+}$ and $(BF_6)^{2-}$ and packed in the way shown in the Figure 1.

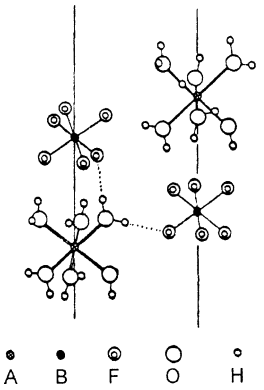

Figure 1. Two neighboring columns in the structure of $ABF_6 \cdot 6H_2O$ crystals.[2]

In terms of their structure the fluosilicates can be divided into two groups; the symmetry of high-temperature phases for crystals with A = Ni, Zn, Co is determined as $R\bar{3}$[7,9] and, respectively, as $R\bar{3}m$, $P\bar{3}m1$, $P\bar{3}$ for those with A = Fe, Mn, Mg.[4,6,10,14,15] All fluosilicates except nickel and zinc undergo improper ferroelastic phase transitions that lead to the monoclinic $P2_1/c$ system.[13] The mechanism of transitions is described in terms of rotations of the metal−water and fluosilicate octahedra in the neighboring columns.

From the calorimetric data it has been found that values of the entropy change $\Delta S/R$ at the phase transitions are different for these two groups of crystals; large values 0.7 or higher are characteristic for the first group, and rather small values less than 0.5 are characteristic for the second one.[11,12]

The high-temperature structure of the $MgSiF_6 \cdot 6H_2O$ is closely related to that of the low-temperature phase.[4] The structural model of the high-temperature phase of $MgSiF_6 \cdot 6H_2O$[4] involves an arrangement of two types of ordered domains (the space group $P\bar{3}$) built from the low-temperature cell, that take the form

* E-mail: zapart@mim.pcz.czest.pl.

10.1021/jp020560f CCC: $25.00 © 2003 American Chemical Society
Published on Web 04/04/2003

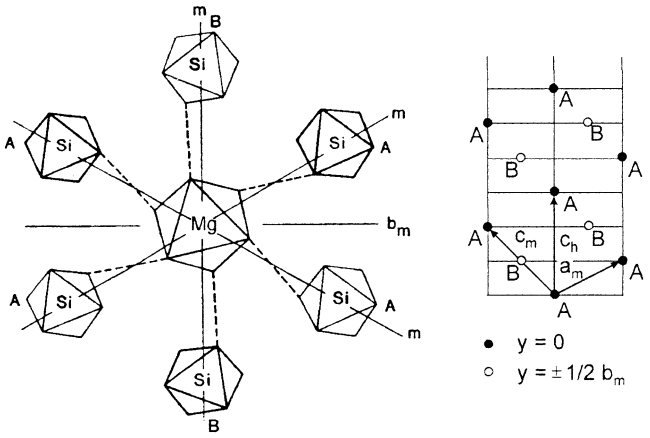

Figure 2. (a) The arrangement of anions (labeled Si) surrounding a cation (labeled Mg) in $MgSiF_6 \cdot 6H_2O$ as viewed down the pseudohexagonal axis c_h in the low-temperature monoclinic phase, (b) the ordering of the two configurations A and B of one kind of octahedral complex ion in projection onto the pseudohexagonal $(1\bar{2}.0)$ plane (adapted from ref 13). The B orientations are related to the A orientations by reflections in the mirror planes labeled by *m*.

of layers parallel to the hexagonal basal plane. Figure 2a shows the arrangement of $(SiF_6)^{2-}$ anions surrounding the $[Mg(H_2O)_6]^{2+}$ cation in the monoclinic phase. For clarity, the $[SiF_6]^{2-}$ octahedra above and below the cation have been omitted. This figure shows the two different orientations, labeled A and B, of the fluosilicate octahedra that are related to each other either by a rotation around the pseudohexagonal axis c_h or reflection in the mirror planes (marked by m) of the trigonal structure. Similarly, there are also two different orientations of the magnesium octahedra. The orientational order with alternate layers ABAB... perpendicular to the monoclinic b_m axis in the monoclinic phase is shown in Figure 2b. The other kind of complex ion is located in the same columns parallel to the c_h axis as the ions shown and halfway between them.

The structural model of the high-temperature phase of $MgSiF_6 \cdot 6H_2O$ is based on a periodic alternation of elements of the low-temperature structure $P2_1/c$. It involves the presence of two types of ordered domains with equal volume parts. The structure is described with a hexagonal cell (space group $P\bar{3}$) consisting of one octahedron of B orientation and two octahedra of A orientation (domain I). For the second domain II the situation is reversed. Figure 3 depicts the ordering of these inequivalent orientations, for one kind of the octahedral complex ion only ($[SiF_6]^{2-}$), in the high-temperature phase. The other kind lies in the same columns along the hexagonal axis c_h, separated from their neighbors in the c_h direction by $\pm c_h$ (Figure 1). For each kind of octahedral ions, one type of domain contains two orientations A for each orientation B; the situation is reversed in the other type of domain. The overall stacking order along the c_h axis is AABAABABBABBAAB.... Thus, the whole structure is made up of a coherent modulated arrangement of elements of the monoclinic structure that are commensurate with the lattice.[4]

EPR OF Mn^{2+} in Magnesium Fluosilicate

The EPR spectra of Mn^{2+} ions consist of five fine structure components that are divided into six lines of hyperfine structure. The EPR studies of Mn^{2+} ions substituting the Mg^{2+} sites in the MFSH crystal[5] confirmed an occurrence of the ferroelastic phase transition at $T_c = 298$ K and revealed a very interesting behavior of the EPR spectra in the high-temperature phase. In

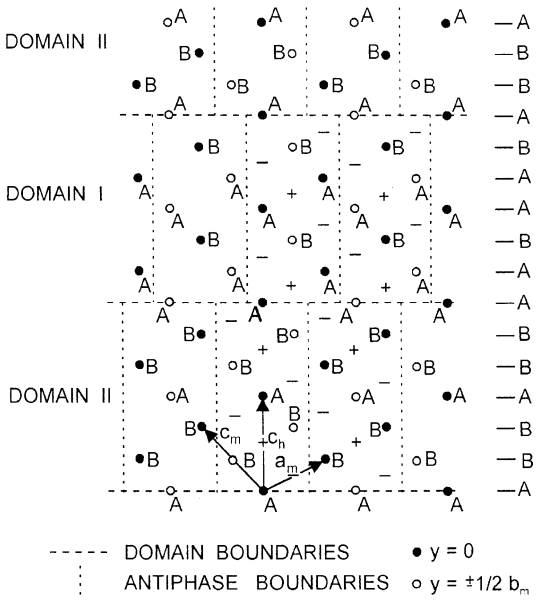

Figure 3. The arrangement of the two orientational configurations A and B of the species of octahedral complex ion in the high-temperature phase of MFSH ($T > 300$ K). The projections onto the hexagonal plane $(1\bar{2}.0)$ which contains the c_h axis as well as the monoclinic a_m and c_m axes. The elements of the low-temperature monoclinic structure arranged periodically in antiphase within each domain are shown.[4]

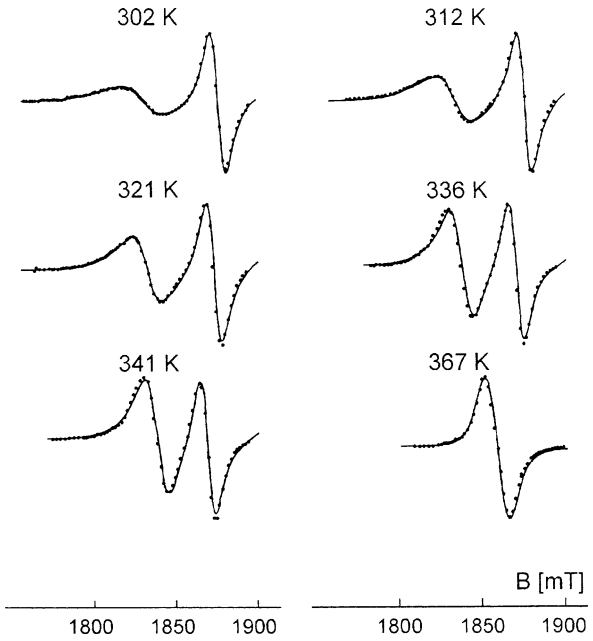

Figure 4. Temperature evolution of the EPR line shape in MFSH. Points, experimental spectra; solid line, simulated spectra.

the temperature range of 345 −370 K, the broadening of each line of the outer fine structure transitions was found along with a gradual splitting of the line observed below 345 K**.** The temperature evolution of EPR lines of the low field Mn^{2+} hyperfine line $|-5/2, m> \leftrightarrow |-3/2, m>$ in MFSH in the high-temperature phase is shown in Figure 4 (marked by the dotted line). It was found[5] that the narrower line of the two-peak spectrum is of the Lorentzian shape and its width does not change, whereas the width of the second much broader line increases with decreasing temperature.

The EPR spectra were interpreted in the framework of an incommensurately modulated structure.[5,16] Although this model gives a good fit of both the experimental and simulated lines,

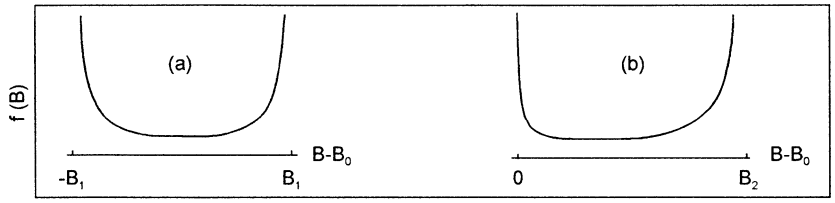

Figure 5. Distribution function against $B - B_0$ for linear (a) and quadratic (b) cases.

it is in a disagreement with the structural studies. Since neither X-ray nor neutron diffraction studies have revealed any presence of superstructure reflections in incommensurate positions, the interpretation of the EPR line shapes in this crystal in the framework of regular antiphase domain structure has been undertaken.

Continuous and Discrete Antiphase Domain Wall Models

The ability to observe signals from the paramagnetic centers lying in the domain walls was reported in paper.[17] In such a case the EPR lines from the centers lying in the domain walls overlap with the EPR lines from centers lying inside the domains. As a result the total spectrum forms a broad continuum limited by two edge singularities. Such a spectrum resembles the one observed in the incommensurate phases.[18] The basic theory describing the spectrum in the case of antiphase domain structures was given in refs 19,20.

The considered continuous domain wall model is based on the assumption that the antiphase boundaries have a linear structure that is represented by the kink-like solution:

$$Q(x) = Q_o \tanh(kx) \tag{1}$$

where k^{-1} is the measure of domain wall thickness, the x-axis is normal to the APB plane, and Q_o is the value of the order parameter inside the two domains. If the resonance field can be expanded into the power series of the order parameter then this field is given by formula

$$B = B_0 + A_1Q + A_2Q^2 + ... \tag{2}$$

where B_0 is a magnetic resonance field in the absence of the order parameter Q.

From eqs 1 and 2 it follows

$$B = B_0 + B_1 \tanh(kx) + B_2 \tanh^2(kx) + ... \tag{3}$$

The coefficients B_1 and B_2 depend on the symmetry of the paramagnetic center site and the direction of the external magnetic field with respect to the symmetry elements of the crystal lattice. The resonance field distribution function $f(B)$ that determines the EPR line shape is given by

$$f(B) = 2\pi/(\mathrm{d}B/\mathrm{d}x) \tag{4}$$

The overall EPR line shape $F(B)$ is given by convoluting the resonance field distribution function $f(B)$ with the line shape function $L(B - B_c)$ of a single line:

$$F(B) = \int L(B - B_c)\, f(B_c)\, \mathrm{d}B_c \tag{5}$$

The zeros of the derivative dB/dx in eq 4 determine the singularities in the line shape. Let us consider some special cases.

(a) When the linear term in eq 3 is dominant ($B_1 \neq 0$, $B_2 = 0$). Then the resonance field distribution function $f(B)$ becomes

$$f(B) = (2\pi/k)\frac{\cosh^2(kx)}{B_1} = \frac{2\pi/k}{\left[B_1 - \dfrac{(B - B_0)^2}{B_1}\right]} \tag{6}$$

We find that it has the characteristic edge singularities at two values of the magnetic field,

$$B_{\pm} = B_0 \pm B_1 \tag{7}$$

Figure 5a shows a plot of the above function against $(B - B_0)$.

(b) When the quadratic term is dominant. Here, ($B_1 = 0$ and $B2 \neq 0$) eq 4 becomes

$$f(B) = \frac{2\pi \cosh^2(kx)}{B_2 k \tanh(kx)} = \frac{2\pi/k}{2B_2\sqrt{\dfrac{(B - B_0)}{B_2}\left(1 - \dfrac{(B - B_0)}{B_2}\right)}} \tag{8}$$

Figure 5b presents a plot of the $f(B)$ in the quadratic case. It is worth noting that now $f(B)$ is asymmetric in shape. There are two singularities at

$$B = B_0 \text{ and } B = B_0 + B_2 \tag{9}$$

The position of one singularity represents a continuation of the para-phase line at $B = B_0$.

For a magnetic field parallel to the 3-fold axis of the crystal the power series (eq 3) contains only even terms and the function $f(B)$ is given by eq 8; it allows one to obtain the simulated EPR lines**.** Figure 6 presents a comparison between the simulated and experimental lines for Mn^{2+} centers in $Mg(SiF_6)\cdot 6H_2O$.

Although the above model with a continuous variable allows us to predict the splitting of resonance lines and changes in the EPR line shape, it does not ensure good agreement between the experimental and theoretical lines in a whole temperature range. According to the structural model,[4] the domain width is comparable with the size of unit cell and the transient region (domain wall) is a result of the error in the stacking of only the single plane, e.g., the first plane A in domain I in Figure 3. Therefore the discrete domain wall model rather than the continuous one should be used to describe the observed EPR spectra in MFSH.

In the high-temperature phase one could recognize two kinds of the $[Mg\cdot 6H_2O]$ centers—one situated inside the antiphase domain in positions with the inversion symmetry and another one located near the domain boundary in positions without this symmetry element.[20,21] The coordination neighborhood of the latter belongs to the two adjacent domains, hence one can assume that this kind of center is situated within a thin domain

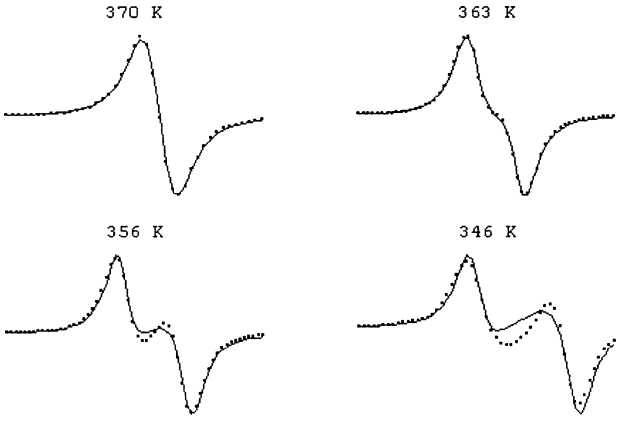

Figure 6. The comparison between experimental (dotted line) and simulated (solid line) EPR line shape in the case of the continuous domain wall model.

TABLE 1: Fitting Parameters of the Calculated EPR Spectra

T [K]	B_{1res} [mT]	ΔB_{1p-p} [mT]	B_{2res} [mT]	ΔB_{2p-p} [mT]
302	188.35	1.02	183.35	3.12
312	188.3	1.02	183.35	2.48
321	188.0	1.0	183.5	2.08
336	187.65	1.0	183.95	1.6
341	187.5	1.0	184.05	1.56

wall. The thickness of this domain wall is equal to the distance between the two nearest planes (e.g., AA in Figure 3).

The manganese ions could incorporate into these two sites (with and without the inversion symmetry), thus giving out two different paramagnetic complexes that can be seen as two different resonance lines in the EPR spectra. In this model any changes in the domain thickness should lead to changes in the relative intensity of these resonance lines.

Discussion

In the HT phase each Mg ion occupies a site with the 3-fold rotational symmetry. It can be seen from Figure 3 that these sites are not all identical; some of them have the inversion symmetry (marked by "+") while others do not (marked by "−"). The centers "+" are localized inside the domains while those marked "−" are near the boundaries. The manganese ions built into these sites can give structurally different paramagnetic complexes that can be seen in the EPR spectra as splitting of the resonance lines. Thus the broad EPR line could be regarded as having originated from the centers "−" and the narrow one from "+" centers. As they are distributed throughout the crystal with the ratio 2:1, the total intensity of the EPR lines should give such a ratio. The simulated EPR spectra in the temperature range 302−341 K are fitted for such a value (Figure 4). Fitting parameters of the simulated spectra are given in Table 1, where B_{1res} and B_{2res} are the positions of these two resonance lines and ΔB_{1p-p} and ΔB_{2p-p} their widths, respectively.

What is more, three kinds of centers without the inversion symmetry can be recognized. The SiF_6 groups that form the 8-fold coordination of the Mg−water complex are depicted in the Figure 7. Their ordering alongside the 3-fold axis of the crystal is given as ABBA (and alternatively BAAB) for the sites "+" (Figure 7a) and as BABA, AABB, and AABA for the sites "−" (Figure 7b−d). Therefore three kinds of paramagnetic centers in positions "−" should be present in the HT phase. Their relative occupation is 6:1:1. Assuming that the positions of the EPR lines from these centers are only slightly different one could speculate that these centers could be seen as one broad line. It was also assumed that these three component lines possessed the same width as the second narrow line (from "+" centers).

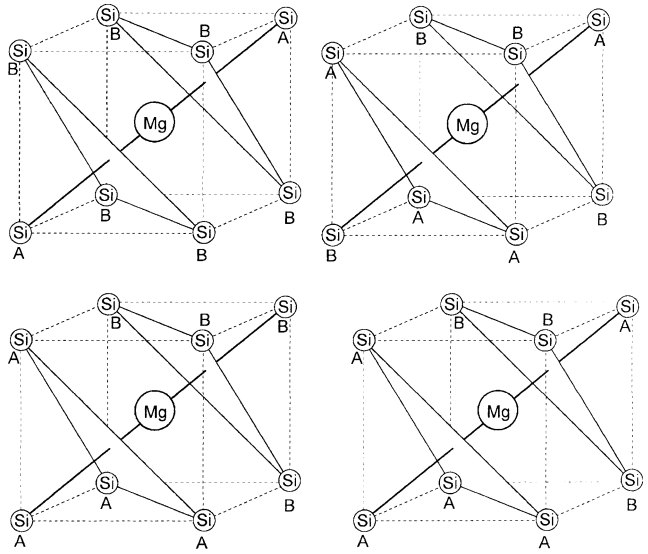

Figure 7. The arrangement of anions (labeled Si) surrounding a cation (labeled Mg) in MSFH as viewed along the 3-fold axis in the high-temperature phase. The ordering of the A and B configurations for centers with (a) and without (b−d) inversion symmetry is shown.

However, for the relations 6:1:1 it was not possible to reproduce the width and the shape of this broad line. Hence one can suggest that the difference in the relaxation time for the centers lying in the "+" and "−" positions results in the difference of the width of EPR lines of these two centers.

Figure 7 presents the model of the deformation of the crystal structure inside the domains and in the domain walls according to refs 4,15. The crystal field acting on the paramagnetic centers is usually given in the form of series of spherical harmonics:

$$V = \sum_{n,m} A_n{}^m r^n Y_n{}^m(\theta,\varphi) = V_{odd} + V_e \qquad (10)$$

where n is smaller than or equal to 4 for the d-electrons and θ and φ are the coordinates of electron. In the above expression, V_{odd} and V_e are the odd and even terms in the power series. In the simplest version of the crystal field theory the even terms are responsible for the values of the spin Hamiltonian parameters and the spin−lattice relaxation time. It turns out that the odd terms become significant in the crystal field theory if one takes into account admixtures of the excited states. The odd terms could change not only the spin Hamiltonian parameters but the spin−lattice relaxation time as well.

From the model of the crystal structure deformation as presented in Figure 7, it follows that the even terms of the crystal field are the same for both the centers from the domains as well as domain walls. So the small difference between the positions of the narrow and broad EPR lines could be attributed to the influence of the odd terms on the spin Hamiltonian parameters.

Moreover, the influence of the odd terms results in a significant increase of the spin−lattice relaxation time for the centers lying in positions without the inversion symmetry as compared to the spin−lattice relaxation time for the centers with the inversion symmetry. The above process leads to broadening of the EPR lines originating from the centers without the inversion symmetry, i.e., those lying in the domain walls.

Such a broadening of the EPR lines has been described in ref 22 where paramagnetic centers either with or without an

inversion symmetry occurred in different crystals, but never both at the same time. In $MgSiF_6.6H_2O$ such centers (marked here as "+" and "−") are found in the very same crystal coexisting together and moreover, the magnitude of the crystal field deformation for these two kinds of centers is the same. The investigation that tries to find relations between changes in the spin Hamiltonian parameters and relaxation times for the manganese centers in this crystal is now in progress.

It is worth noticing that the structure of the antiphase domain wall, as seen from the EPR investigations, is also consistent with the theoretical models of domain walls presented in paper.[23] It has been shown that the central part of the domain walls should possess a symmetry different from that in the domain. In particular, if the domain possesses a center of inversion, the central part of the domain wall should not possess it at all.

Taking it into account, the simulated EPR spectrum was approximated by two lines: the narrow one and another one much broader as shown in the Figure 4.

The above model stops working in the vicinity of temperature 350 K. The crystal begins to lose the crystalline water around this temperature,[24] which would lead to significant changes of the EPR spectrum.

Acknowledgment. The author thanks Prof. A. M. Ziatdinov for supplying the experimental EPR spectra.

References and Notes

(1) Fujiwara, K. *J. Phys. Soc. Jpn*. **1957**, *12*, 7.
(2) Jehanno, G.; Perio, P. *J. Phys. France* **1962**, *23*, 854.
(3) Bak, P. *Rep. Prog. Phys*. **1982**, *45*, 587.
(4) Chevrier, G.; Jehanno, G. *Acta Crystallogr. A* **1979**, *35*, 912.
(5) Ziatdinov, A. M.; Kuryavyi, V. G.; Davidovich, R. L. *Sov. Phys. Solid State* **1985**, *27*, 1288; Ziatdinov, A. M.; Kuryavyi, V. G. *Ferroelectrics* **1993**, *143*, 99.
(6) Hamilton, W. C. *Acta Crystallogr*. **1962**, *15*, 353.
(7) Bose, M.; Roy, K.; Ghoshray, A. *Phys. Rev. B* **1987**, *35*, 6619.
(8) Ghosh, B.; Chattarjee, N.; Das, A. N.; Chatterjee, A. *J. Phys. C* **1979**, *12*, 3283.
(9) Ray, S.; Zalkin, A.; Templeton, D. H. *Acta Crystallogr. B* **1973**, *29*, 2741; Ray, S.; Mostafa, G. *Z. Kristallogr*. **1996**, *211*, 368.
(10) Kodera, E.; Torii, A.; Osaki, K.; Watanabe, T. *J. Phys. Soc. Jpn*. **1972**, *32*, 863.
(11) Weir, R. D.; Halstead, K. E.; Staveley, L. A. K. *Discuss. Faraday Soc*. **1980**, *69*, 202; *J. Chem. Soc. Faraday Trans. 2* **1985**, *81*, 189.
(12) Flerov, I. N.; Gorev, M. V.; Aleksandrov, K. S.; Afanasjev, M. L. *J. Phys.: Condens. Matter* **1992**, *4*, 91.
(13) Syoyama, S.; Osaki, K. *Acta Crystallogr. B* **1972**, *28*, 2626.
(14) Jehanno, G.; Varret, F. *Acta Crystallogr. A* **1975**, *31*, 857.
(15) Chevrier, G.; Jehanno, G. *Acta Crystallogr. A* **1981**, *37*, 578.
(16) Skrylnik, P. G.; Ziatdinov, A. M. *Bull. Magn. Res*. **1999**, *19*−*20*, 83.
(17) Zapart, M. B.; Zapart, W.; Jang, M. S.; Jeong, S. Y. *Ferroelectrics* **1995**, *172*, 437.
(18) Zapart, M. B.; Snoeck, E.; Saint-Gregoire, P. *Ferroelectrics* **1997**, *191*, 179.
(19) Zapart, W.; Zapart, M. B. *Bull. Magn. Reson.* **1999**, *19*, 34.
(20) Zapart, W.; Zapart, M. B. *Ferroelectrics* **2000**, *240*, 101.
(21) Price, D. C. *Can. J. Phys.* **1987**, *65*, 1280.
(22) Glinchuk, M. D.; Gratchev, W. G.; Deigen, M. F.; Roitsyn, A. B.; Suslin, L. A. *Elektriczeskije Effekty w Radiospektroskopii*, Nauka, Moskva, 1981, and citations therein.
(23) Privratska, J.; Janovec, V.; Machonsky, L. *Ferroelectrics* **2000**, *240*, 83.
(24) Flerov, I. N.,; Gorev, M. V.; Melnikova, S. V.; Afanasjev, M. L.; Aleksandrov, K. S. *Fiz. Tverd. Tela* **1991**, *33*, 1921.